Preprint
UCRL-JC-149106

Interferometric Diagnosis of Two-Dimensional Plasma Expansion

R. F. Smith, S. Moon, J. Dunn, J. Nilsen, V. N. Shlyaptsev, J. R. Hunter, J. Rocca, J. Filevich, M. C. Marconi

This article was submitted to
8th International Conference on X-ray Lasers, Aspen, CO., May 27-31, 2002

July 31, 2002

U.S. Department of Energy

Lawrence
Livermore
National
Laboratory

This work was performed under the auspices of the United States Department of Energy by the University of California, Lawrence Livermore National Laboratory under contract No. W-7405-Eng-48.

Interferometric Diagnosis of Two-Dimensional Plasma Expansion

Raymond F. Smith[1], Steven Moon[1], James Dunn[1], Joseph Nilsen[1], Vyacheslev N. Shlyaptsev[1], James R. Hunter[1], Jorge Rocca[3], Jorge Filevich[3], Mario C. Marconi[3, 4]

[1]*Lawrence Livermore National Laboratory, Livermore, CA 94551*
[2]*University of California Davis-Livermore, Livermore, CA 94551*
[3]*Dept. of Electrical and Computer Engineering, Colorado State University, Fort Collins, CO 80523*
[4]*Physics Dept., University of Buenos Aires, Argentina*

Abstract. Recent advances in interferometry has allowed for the characterization of the electron density expansion within a laser produced plasma to within 10 μm of the target surface and over picosecond timescales. This technique employs the high brightness output of the transient gain Ni-like Pd collisional x-ray laser at 14.7 nm to construct an effective moving picture of the two-dimensional (2-D) expansion within the plasma. In this paper we present experimentally measured density profiles from an Al plasma and make comparisons with 1.5-D and 2-D code simulations. The results are discussed along with an analysis of the underlying mechanisms driving the plasma expansion.

1. INTRODUCTION

Interferometry is a powerful tool for accurately diagnosing the two-dimensional (2-D) evolution of dense laser-produced plasmas. For fast evolving plasmas it is desirable that the duration of the probe pulse is short to obtain an effective snapshot of the density profile while reducing the effects of plasma motion blurring at the ablation front. The picosecond duration and short wavelength of the 14.7 nm Ni-like Pd laser mitigates effects associated with motion blurring and refraction through millimeter scale plasmas. This enables direct measurement of the electron density profile to within 10 μm of the target surface [1]. A series of high quality 2-D density measurements provide unambiguous characterization of the time evolution in a fast evolving plasma suitable for validation of existing 1-D and 2-D hydrodynamic codes. The electron density evolution of a laser-heated Al plasma is measured using a diffraction grating interferometer (DGI) [2] at different times, relative to the peak of the plasma forming pulse. The experimental results are compared with 1.5-D and 2-D hydrodynamic simulations in order to further our understanding of the mechanisms driving plasma expansion.

2. EXPERIMENTAL RESULTS

The Ni-like Pd 14.7 nm x-ray laser probe beam and the plasma to be studied were generated using three laser beams at 1054 nm wavelength from the COMET facility at LLNL [1]. Single pass saturated x-ray laser output of a few 10's of μJs was achieved with an optical pumping combination of a 600 ps long pulse (2 J, 2×10^{11} W cm^{-2}) and a 6 ps (5 J, 7×10^{13} W cm^{-2}) main heating pulse. The x-ray laser output was imaged and routed into a diffraction grating interferometer for plasma probing experiments. For details of the instrumentation see ref [1, 2].

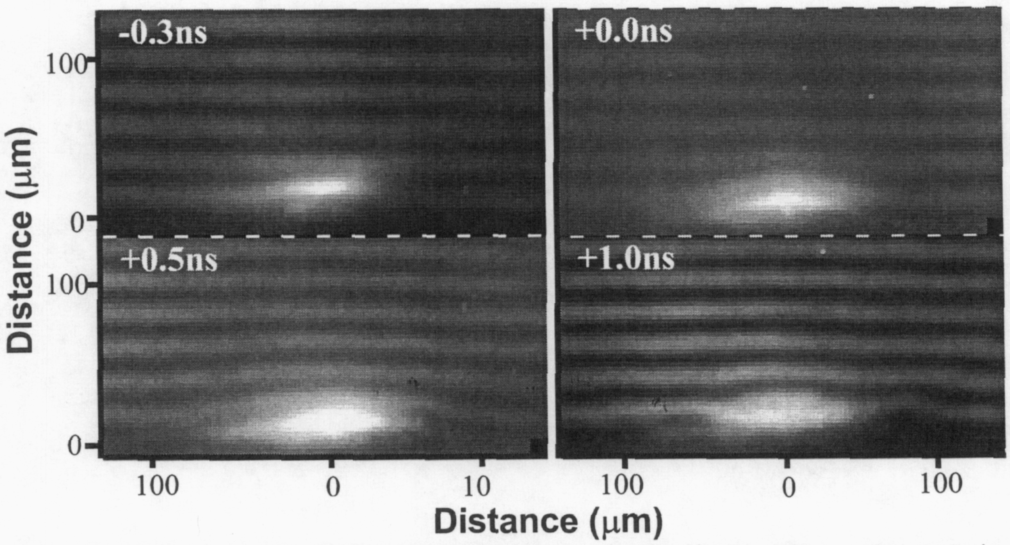

Figure 1. Interferograms representing 2-D electron density profiles for different times relative to the peak of the 600ps plasma forming pulse.

A plasma heated by up to 2 J of energy in a 600 ps, 1054 nm pulse, corresponding to a maximum intensity of 3×10^{12} W cm^{-2}, was produced in one arm of the interferometer. A 6 mm long line focus with a 20 μm focal width, was generated on a polished 1mm long Al slab target using a combination of a cylindrical lens, f = -200 cm, and an off-axis paraboloid, f = 30 cm. The relative delay between the arrival of the x-ray laser probe pulse, represented by the short pulse beam, to the peak of the plasma forming beam was measured to within 100 ps with a fast diode. The x-ray laser could probe the plasma in the temporal range of –1 ns to +2 ns relative to the peak of the 600 ps plasma forming pulse by adjusting a delay arm in the plasma laser beam. The line focus plasma was probed longitudinally by the x-ray laser, thereby minimizing uncertainties in the interpretation of the interferograms arising from plasma gradients along the probe path. The plasma was imaged by a 25 cm focal length spherical multilayer mirror and relayed to a thinned back-illuminated 1024 × 1024 CCD detector with 24 × 24 μm^2 pixels. A 2000 Å Zr/1000 Å Polyimide ($C_{22}H_{10}N_2O_5$) filter was placed in front of the CCD to block visible and UV light. The magnification of the imaging system was determined to be 9.94, by imaging a fine mesh at the target plane, giving a pixel-limited spatial resolution of 2.55 μm. The target angle was determined to be parallel to the x-ray laser beam to better than ± 0.25°. Using the x-ray laser beam with no plasma present, high quality fringes, with visibility $V = (I_{max} - I_{min})/(I_{max} + I_{min})$ of 0.72 ± 0.12, were observed for a 700 × 500 μm² (H × V) region indicating excellent spatial coherence in the laser beam. Figure 1 shows a series of interferograms at different probing times relative to the peak of the plasma forming pulse. The electron density, n_e in cm^{-3}, is related to the measured fringe shifts as $N_{fringe} = 6.68 \times 10^{-20}\, n_e\, L$, where L is the length (cm) of the plasma being probed by the 14.7 nm x-ray laser [3].

Significant lateral expansion from the initial 20 μm focal width is observed at all times with the expansion velocity parallel to the target surface measured to be 7.5×10^6 cm/s over the interval of probing. This is in agreement with the expected sound speed for a plasma electron temperature of $T_e \sim 80$ eV. For all the interferograms the sideways expansion is symmetrical about the center of the focusing region. A lot of structure is observed less than 10 μm from the target surface at the limit of the spatial resolution of the imaging system. At 1 ns after the peak of the plasma forming pulse we observed off-axis density enhanced lobes close to the target surface and at approximately 80 μm either side of the central region. In addition, perturbations in the fringes away from the target surface indicated an expansion angle of ± 35° at t > 0.5 ns.

3. SIMULATIONS

Figure 2(a) shows the experimentally observed on-axis electron density profile for different probing times. It can be seen at early times, t = -0.3 ns and 0 ns, that the density scale-length is short and the plasma has expanded to 60 μm from the initial target surface. At later times, t = +0.7 ns and 1.0 ns when the plasma heating pulse is effectively off, the plasma scale-length has relaxed and the plasma has continued to expand to 160 μm. Analysis considering the effects of refraction [4] has shown a 20% uncertainty in the highest density measurements. The lowest measured electron density for this target length is limited to 2×10^{18} cm^{-3} and is dependent on the minimum detection of the fringe shift. The error bars on the density measurement in Figure 2(a) represent the uncertainty in determining the position of the fringes.

Alongside these measurements are the predicted electron density values from the 1.5-D LASNEX [5] plasma physics code. The LASNEX simulations are one-dimensional but include an expansion angle of 15 degrees in the direction perpendicular to the primary expansion (1.5-D) so as to simulate the 2-D effects associated with the narrow width of the line focus on the target. The code predictions give qualitatively good agreement in reproducing the plasma density profile evolution. The overall trend, however, is for the simulations to show somewhat higher density at all times. The predicted n_e values increase rapidly within 5 μm of the target surface. Experimental images indicate very fine fringe structure in this region, which are not well resolved by our present imaging setup. Within our current experimental setup, this has proved to be the limit on the maximum diagnosable electron density. This however does not represent the limit of the technique. The critical density for the 14.7

nm probe wavelength is 5×10^{24} cm^{-3} and gives the ultimate limit to the density with which the x-ray laser can probe. By optimizing the instrumentation and plasma conditions we expect to closer approach this figure in future experimental work.

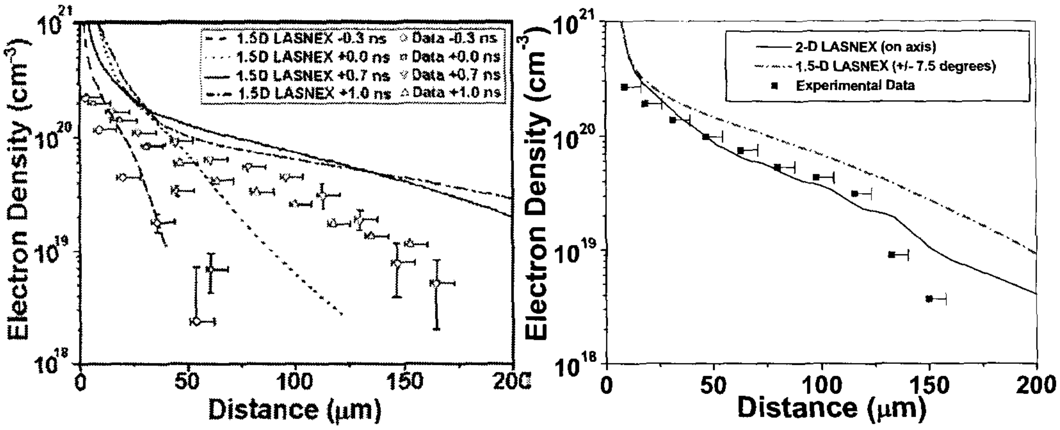

Figure 2 (a) 1-D on axis density slices from experimentally obtained interferograms compared with profiles predicted by 1.5-D LASNEX simulations. (b) Comparison of on axis density from 2-D and 1.5-D (± 7.5°) LASNEX simulations with experimentally obtained electron density measurements at t = 0.5 ns.

Figure 2(b) shows the experimentally determined electron density as a function of distance away from the target surface taken 0.5 ns after the peak of the plasma forming pulse. Also shown is the predicted on axis electron density from the LASNEX 1.5-D (± 7.5°) and 2-D simulations. It is clear that there is better agreement for the latter. For the 1.5-D case, all the ablated mass is artificially confined to a fixed cone angle of expansion, an approximation which, in the case of significant lateral expansion, will increase the predicted on-axis density. It has been found that by increasing the cone angle within the 1.5-D simulations improved agreement with experiment is obtained.

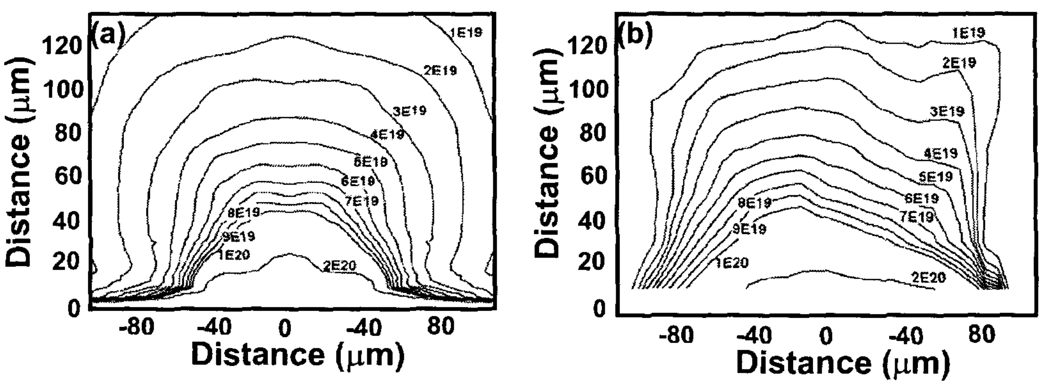

Figure 3 (a) Simulated 2-D electron density profile using LASNEX. (b) Measured 2-D electron density profile 0.5 ns after the peak of the 600ps duration plasma forming beam. The error bars for distance away from the target are –2 μm, + 8 μm.

Figure 3 shows a contour plot of a 2-D LASNEX [4] simulation and the corresponding experimental data at $\Delta t = 0.5$ ns with good quantitative agreement. Such modeling covers all phases of expansion leading to a plasma size much larger than the focal spot. To understand the mechanisms driving the expansion of the plasma it is necessary to track the evolution of the plasma parameters. Figure 4(a) shows the calculated 2-D electron temperature and density profile at the peak of the 600 ps plasma forming beam. It is predicted that there exists a hot (~150 eV) on-axis region close to the critical surface of the 1ω driver. The temperature gradients relax slowly in the plane of primary expansion. However there are steep gradients in the lateral direction. The plasma close to the target is calculated to be relatively cold (~40 eV) just outside the 20 μm FWHM of the laser driver. An electron density contour map is also shown on the same plot. It is seen that at the peak of the pulse a rippling of the critical density surface is predicted, with side lobes developing at low temperatures at approximately 20 μm off-axis. In figure 4(b) a momentum vector map illustrates that there is a significant lateral push of mass from these side lobe regions in the direction away from the center of the focusing beam.

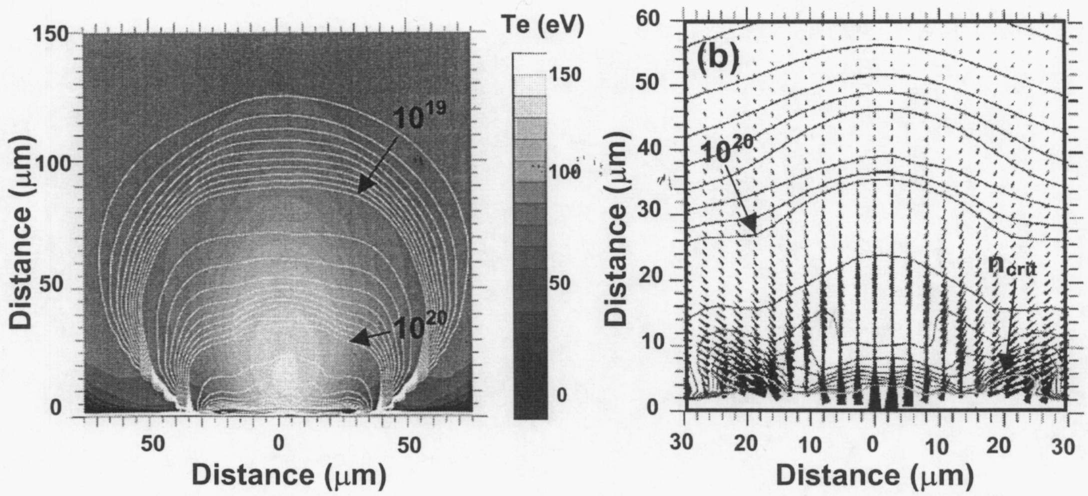

Figure 4 (a) Electron density and electron temperature contours at the peak of the plasma forming pulse [$\Delta t = 0$ ns] (b) Momentum vector plot at the same time.

4. CONCLUSIONS

Picosecond x-ray laser interferometry is a valuable technique in diagnosing plasma evolution within laser produced plasmas. The short sampling time of the probe beam reduces blurring effects and allows for probing to within 10μm of the target surface. In addition, the short wavelength probe minimizes effects associated with refraction and free-free absorption making this diagnostic well suited for studying large, fast evolving, dense plasmas. It has been shown that for the experimental conditions reported within this paper lateral expansion is a significant effect. Two-dimensional plasma physics codes are therefore necessary to model such experiments. Preliminary simulations have indicated that cool dense and relatively slow moving regions, which lie outside of the full width at half maximum (FWHM) of the laser focus, drive the lateral expansion. Future work will focus on understanding the dominant energy transport mechanisms, which drive the plasma expansion.

ACKNOWLEDGEMENTS

The support of Al Osterheld and Andy Hazi is greatly appreciated. The authors are pleased to acknowledge the technical contributions from Carl Bruns and Al Ellis. This work was performed under the auspices of the U.S. Dept. of Energy by the University of California Lawrence Livermore National Laboratory, through the Institute for Laser Science and Applications, under Contract No. W-7405-Eng-48 and by US Department of Energy Grant No. DE-FG03-98DP00208. The development of the interferometer gratings was supported with a grant from the State of Colorado Photonics and Optoelectronics program.

REFERENCES

1. R.F. Smith, J.Dunn, J. Nilsen, V.N. Shlyaptsev, S. Moon, J. Filevich, J.J. Rocca, M.C. Marconi, J.R. Hunter, and T.W. Barbee, Jr., Phys. Rev. Lett., **89** (6), 065004-1 (2002).
2. J. Filevich, K. Kanizay, M. C. Marconi, J. L. A. Chilla, and J. J. Rocca, Opt. Lett. **25**, 356-357 (2000).
3. L. B. Da Silva, T. W. Barbee, Jr., R. Cauble, P. Celliers, D. Ciarlo, S. Libby, R. A. London, D. Matthews, S. Mrowka, J. C. Moreno, D. Ress, J. E. Trebes, A. S. Wan, and F. Weber, Phys. Rev. Lett. **74**, 3991-3994 (1995).
4. R.F. Smith, V.N. Shlyaptsev, J. Dunn, J. Nilsen, J.R. Hunter, J.J. Rocca and J. Filevich, M.C. Marconi, "Refraction Effects on X-ray and UV Interferometric Probing of Laser Produced Plasmas" submitted for publication to JOSAB (2002).
5. G.B Zimmerman and W.L. Kruer, Comments Plasma Phys. Controlled Fusion **2**, 51-61 (1975).